Bromopalladates(II) of Xanthine Derivatives. Crystal Structure of 1,3,8-Trimethylxanthinium Tribromopalladate(II) Monohydrate

MARISA I. MORENO-VIDA, ENRIQUE COLACIO-RODRIGUEZ, MIGUEL N. MORENO-CARRETERO, JUAN M. SALAS-PEREGRIN*

Departamento de Química Inorganica, Facultad de Ciencias, Universidad de Granada, 18071 Granada, Spain

MICHEL SIMARD and ANDRÉ L. BEAUCHAMP*

Département de Chimie, Université de Montréal, C.P. 6128, Succ. 'A', Montreal, Que., H3C 3J7, Canada

(Received July 19, 1988)

Abstract

Reaction of $PdBr_2$ in aqueous HBr yielded salts of the type $(LH)_2[PdBr_4]$ for L = theobromine and theophylline, and $(LH)_2[Pd_2Br_6]$ for L = caffeine and various 1,3-dimethyl-8-alkylxanthines. Crystals of (1,3,8-trimethylxanthinium)$_2[Pd_2Br_6]$ belong to the monoclinic $P2_1/c$ space group, with a = 11.343(2), b = 7.237(1), c = 18.847(4) Å, β = 104.26(1)° and Z = 4. The structure was refined on 2439 independent Cu Kᾱ reflections to R = 0.046. The unit cell consists of dinuclear $[Pd_2Br_6]^{2-}$ anions containing two bridging Br ligands, and 1,3,8-trimethylxanthinium cations in which hydrogens are bound to both imidazolic nitrogen atoms. The unit cell contains stacks of trimethylxanthinium cation pairs alternating with $[Pd_2Br_6]^{2-}$ anions, whereas water molecules form hydrogen bonds with partners in different stacks. The infrared spectra are consistent with the presence of monoprotonated xanthinium cations and $[PdBr_4]^{2-}$ or $[Pd_2Br_6]^{2-}$ ions in all cases. These salts are found to be strongly acidic and to dissociate into the neutral ligands in DMSO solution.

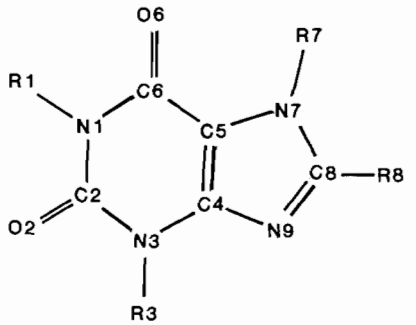

R_1	R_3	R_7	R_8	
H	H	H	H	Xanthine (XH_3)
H	CH_3	CH_3	H	Theobromine (TBH)
CH_3	CH_3	H	H	Theophylline (TFH)
CH_3	CH_3	CH_3	H	Caffeine (CF)
CH_3	CH_3	H	CH_3	1,3,8-Trimethylxanthine (TMH)
CH_3	CH_3	H	C_2H_5	1,3-Dimethyl-8-ethylxanthine (ETH)
CH_3	CH_3	H	C_3H_7	1,3-Dimethyl-8-propylxanthine (PRH)
CH_3	CH_3	H	$CH(CH_3)_2$	1,3-Dimethyl-8-isopropylxanthine (IPRH)

Scheme 1.

Introduction

Considerable effort has been devoted in recent years to the preparation of metal–purine complexes and the structural characterization of the compounds by spectroscopic techniques and X-ray diffraction [1]. Most of this research has been directed toward adenine and guanine molecules, since these residues are components of nucleic acids. Xanthine derivatives have attracted much less attention, in spite of the fact that some of them are present in biological systems and that they may be used as valuable models for biologically important analogues [2]. Some xanthine derivatives also show potential antitumor activities [3].

Most of the literature on complexation with xanthine ligands deals with theophylline (1,3-dimethylxanthine, Scheme 1), for which a number of crystallographic studies have been reported [4–8]. However, X-ray work on complexes with other xanthine derivatives and with xanthine itself is scanty [9–12]. Various groups have worked at determining the metal binding sites in xanthine compounds by using vibrational spectroscopic and NMR techniques [13–18].

As part of our research program on the interactions of metal ions with xanthine ligands [12, 14, 19, 20], we isolated various types of compounds, including normal complexes and xanthinium halometallates, with a number of metals. In the present

*Authors to whom correspondence should be addressed.

0020-1693/89/$3.50

paper, we wish to report on bromo–Pd(II) compounds prepared under acidic conditions with a series of xanthine derivatives (Scheme 1). Among these compounds*, those of the type $(LH)_2[PdBr_4]$ were anticipated to be xanthinium salts of the $[PdBr_4]^{2-}$ anion without direct Pd–xanthine bonding. However, direct interactions, with the carbonyl group for instance, could not be ruled out for the compounds of the $(LH)PdBr_3$ type. This prompted us to examine these compounds in greater detail and to determine the crystal structure for the 1,3,8-trimethyl compound.

Experimental

Instruments and Reagents

Theobromine, theophylline and caffeine were purchased from Carlo Erba. The other purine bases were synthesized in our laboratory following Speer and Raymond [21]. After recrystallization in water, the products were obtained as white crystalline needles.

Microanalyses (C, H, N) were carried out at the Instituto de Quimica Bioorganica (CSIC), Barcelona. Palladium and water were determined gravimetrically using a Mettler TG-50 thermobalance.

IR spectra of the solids were obtained as KBr or polyethylene pellets with a Perkin-Elmer 983G spectrophotometer. The ^1H NMR spectra were taken with a Bruker WH-400 spectrometer using DMSO-d_6 as solvent and TMS as internal standard.

*L is used to represent any of the xanthine derivatives in the neutral form, whereas LH^+ is the corresponding monoprotonated cation.

Preparation of the Compounds

In 50 ml of aqueous HBr solution (0.7 N) containing 100 mg (0.56 mmol) of $PdCl_2$ were dissolved 1.12 mmol of the xanthine derivative. The resulting mixture was heated to 80 °C and stirred for 0.5 h. After a few days, red crystals appeared in all cases. The solids were filtered off, washed with small amounts of ethanol and diethylether, and air dried. The chemical analyses of the compounds are given in Table 1.

Crystal Data

$C_8H_{13}N_4O_3Br_3Pd$, formula weight = 559.33, monoclinic, $P2_1/c$, a = 11.343(2), b = 7.237(1), c = 18.847(4) Å, β = 104.26(2)°, V = 1499.5 Å^3, Z = 4, D_c = 2.477 g cm^{-3}, λ(Cu K$\bar{\alpha}$) = 1.54178 Å (graphite monochromator), μ(Cu Kα) = 198.4 cm^{-1}, T = 170 K, crystal dimensions (mm): 0.03 × 0.07 × 0.44.

Crystallographic Measurements and Structure Determination

The crystal used for X-ray work was an elongated plate obtained as described above. Precession and cone-axis photographs showed only one Laue mirror identifying the monoclinic system. The systematic absences were consistent only with space group $P2_1/c$ ($h0l$, $l \neq 2n$ and $0k0$, $k \neq 2n$).

The same crystal was transferred to the Enraf-Nonius CAD-4 diffractometer. The reduced cell was determined from ten low-angle reflections found on a Polaroid rotation photograph. This cell was then transformed into the conventional monoclinic cell given above. A set of 25 strong reflections in the range $10 \leqslant \theta \leqslant 25$ were centered in the counter aperture. Least-squares refinement of the setting angles of those reflections gave the final cell parameters.

TABLE 1. Analytical Data [Found (Calculated) (%)]

Compound	Formula	C	H	N	Pd
$(TBH_2)_2PdBr_4$	$C_{14}H_{18}Br_4N_8O_4Pd$	21.68 (21.32)	2.23 (2.28)	13.83 (14.21)	12.90 (13.50)
$(TFH_2)_2PdBr_4$	$C_{14}H_{18}Br_4N_8O_4Pd$	21.44 (21.32)	2.26 (2.28)	13.93 (14.21)	13.26 (13.50)
$(CFH)PdBr_3 \cdot 7H_2O$	$C_8H_{25}Br_3N_4O_9Pd$	14.18 (14.39)	2.84 (3.74)	7.62 (8.39)	16.66 (15.95)
$(TMH_2)PdBr_3 \cdot H_2O$	$C_8H_{13}Br_3N_4O_3Pd$	16.70 (17.17)	2.18 (2.32)	9.71 (10.01)	18.49 (19.03)
$(ETH_2)PdBr_3 \cdot H_2O$	$C_9H_{15}Br_3N_4O_3Pd$	18.71 (18.84)	2.74 (2.62)	9.15 (9.77)	18.37 (18.56)
$(PRH_2)PdBr_3 \cdot 2H_2O$	$C_{10}H_{19}Br_3N_4O_4Pd$	19.91 (19.83)	3.02 (3.14)	8.90 (9.25)	17.19 (17.58)
$(IPH_2)PdBr_3 \cdot 2H_2O$	$C_{10}H_{19}Br_3N_4O_4Pd$	20.32 (19.83)	3.07 (3.14)	8.91 (9.25)	17.39 (17.58)

The intensity data were collected following a procedure described elsewhere [22]. Seven standard reflections were monitored during data collection, and their intensity checked every hour showed a fluctuation $< \pm 5.2\%$. Crystal orientation was checked every 100 measurements. The actual position of the scattering vectors and the directions derived from the orientation matrix always differed by $<0.18°$, so that no crystal reorientation was needed during data collection. All *hkl* and $\bar{h}kl$ reflections contained in a sphere limited by $2\theta = 140°$ were collected with graphite-monochromatized Cu K$\bar{\alpha}$ radiation. Among 2839 reflections so obtained, 2439 were retained ($I > 3\sigma(I)$) for structure determination. They were corrected for the Lorentz and polarization effects. An absorption correction was applied (Gaussian integration, grid 10 × 10 × 10, transmission range = 0.11–0.58).

The structure was solved using the SHELX package [23] and refined on $|F_o|$ by full-matrix least-squares. The $PdBr_3$ fragment was found by direct methods. The remaining non-hydrogen atoms were located from a subsequent difference Fourier (ΔF) map phased on the $PdBr_3$ group. Isotropic refinement on the data uncorrected for absorption converged to $R = \Sigma||F_o| - |F_c||/\Sigma|F_o| = 0.122$. The absorption correction reduced R to 0.097. Anisotropic refinement of the known atoms converged to $R = 0.075$. The hydrogen atoms were all visible in the ΔF map. They were introduced at idealized positions (C(N)–H = 1.08 Å, $B = 6.0$ Å^2). The parameters of the hydrogens were not refined, but their coordinates were recalculated after each least-squares cycle. The final residuals obtained at convergence were $R = 0.046$ and $R_w = [\Sigma w(|F_o| - |F_c|)^2/\Sigma w|F_o|^2]^{1/2} = 0.053$. The goodness-of-fit ratio was 1.56. The highest residuals in the ΔF map (2.4–1.3 e/Å) were within 1.1 Å from $PdBr_3$. The ΔF map showed a general background $< \pm 0.9$ e/Å^3.

The scattering factors and anomalous dispersion factors (Hg, Br) were from standard sources [24]. The refined coordinates are listed in Table 2. See also 'Supplementary Material'.

TABLE 2. Refined Fractional Coordinates (×10^4, Pd, Br × 10^5) for $(TMH_2)_2[Pd_2Br_6]\cdot 2H_2O$

Atom	*x*	*y*	*z*
Pd	86178(4)	48417(7)	42886(3)
Br1	92768(7)	41693(13)	55999(4)
Br2	80769(7)	55010(12)	29939(4)
Br3	65387(7)	39691(12)	42464(4)
O2	6645(5)	4861(8)	6997(3)
O6	9903(5)	4374(8)	8955(3)
O10	6045(4)	2451(8)	5805(3)
N1	8248(5)	4591(9)	7986(3)
N3	6305(5)	5485(9)	8110(3)
N7	8187(5)	5711(8)	9891(3)
N9	6275(5)	6243(9)	9375(3)
C2	7031(7)	4980(10)	7666(4)
C4	6817(6)	5688(10)	8843(4)
C5	8012(6)	5315(10)	9149(4)
C6	8821(6)	4747(10)	8739(4)
C8	7146(6)	6270(10)	10011(4)
C11	9014(7)	4122(12)	7494(4)
C31	5015(7)	5963(17)	7813(5)
C81	6970(7)	6856(12)	10730(4)

Results and Discussion

Spectroscopic Results

$PdBr_2$ in 0.7 M aqueous HBr forms with the xanthine derivatives two types of compounds: $(LH)_2[PdBr_4]$ for L = theobromine and theophylline, and $(LH)PdBr_3$ for L = caffeine and the 8-alkyl-1,3-trimethylxanthines. When the structure determination of the 1,3,8-trimethylxanthine compound $(TMH_2)PdBr_3\cdot H_2O$ was undertaken, it made little doubt that the three Br atoms were attached to Pd. However, the entity filling the fourth coordination site could not be unambiguously identified, and the possibility of water or a xanthine carbonyl group being bound to Pd could not be ruled out. The crystallographic results described below show, however, that the compound consists of well separated trimethylxanthinium cations and $[Pd_2Br_6]^{2-}$ anions.

The presence of similar protonated xanthinium ions in the remaining compounds is deduced from solid-state infrared spectroscopy. The spectra of various salts of caffeine have been discussed by Cook and Regnier [25]. Protonation of caffeine introduces two proeminent spectral features: N–H stretching produces a strong massif whose position depends on the counter ion, varying between 2265 (Cl^-) and 3140 (ClO_4^-) cm^{-1}. A weaker and typically broad γ(N–H) band is also detected between 883 (Cl^-) and 724 (ClO_4^-) cm^{-1}. In our $PdBr_3$–caffeine compound, these bands are identified at ~2800 and 880 cm^{-1}, respectively, thereby confirming the presence of the protonated form.

Caffeine is a particularly simple system, because it contains only N–CH_3 groups and the above effects can only be ascribed to the N–H^+ group formed by protonation. The case of theobromine has also been discussed by Cook and Regnier [26], who reported spectral features similar to those of the caffeine salts, but the out-of-plane band could not be unambiguously assigned to the N–H^+ group, because neutral theobromine also gave a band for its N1–H group at this same position. There is no such ambiguity for the remaining derivatives studied here: even if they all possess an N–H group in the neutral state, the N–H^+ bands can still be identified as can be appreciated from Fig. 1, where the regions discussed here are represented for the typical case of 1,3,8-trimethylxanthine. In the neutral compounds, the

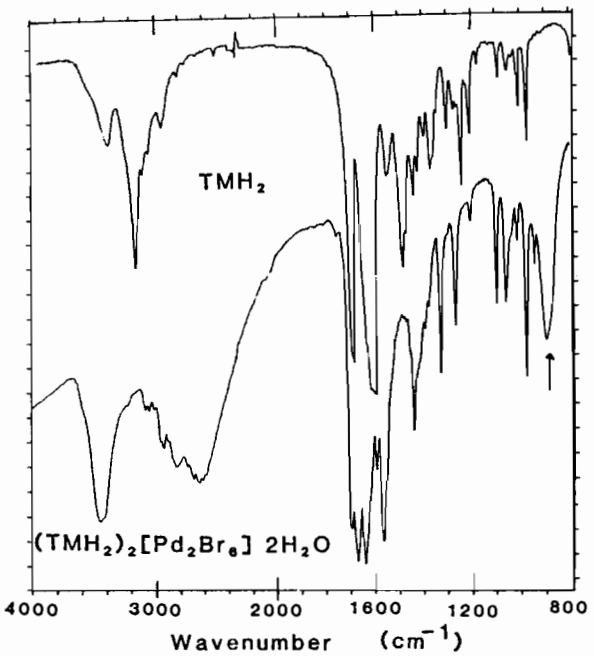

Fig. 1. Portion of the infrared spectra of 1,3,8-trimethylxanthine and its protonated $[Pd_2Br_6]^{2-}$ salt.

ν(N–H) band is sharp and occurs at 3166 cm^{-1}, whereas it probably lies at the same place but it is masked by the strong and very broad N–H^+ band located at ~2700 cm^{-1} in the protonated salts. The well defined absorption at 3460 cm^{-1} is due to the $\nu(H_2O)$ vibration of crystallization water. As to the γ(N–H) vibration, the broad band at 880 cm^{-1} is clearly visible for the protonated species, but no such absorption is present for the neutral derivative. The data for the various compounds are collected in Table 3, and they all show the characteristic pattern for protonation.

Figure 1 also includes the 1500–1700 cm^{-1} region, where double bond stretching vibrations occur. This region is modified in the same characteristic manner for all compounds. The band at highest wavenumber, mainly located in the C2=O2 bond, is not greatly displaced by protonation on the imidazole ring. On the other hand, changes of bond order in the ring and coupling with N–H motion introduce various spectra shifts in the C6=C6 and ring vibrations. This region can also include some contribution from the $\delta(H_2O)$ vibration. Detailed assignment is beyond the scope of the present paper, but the pattern of spectral modifications in this region can be regarded as strong evidence in favor of the protonated form of the xanthine ligand.

The far infrared spectrum also shows a band in the 245–256 cm^{-1} region, which is sufficiently distant from ligand bands to be safely attributed to ν(Pd–Br) [27].

The ^{1}H NMR results for the compounds dissolved in DMSO-d_6 are listed in Table 4. Most of the assignments are based on work by Lichtenberg *et al.* [28] and by Twanmoh *et al.* [29].

Even though the IR spectra indicated the presence of protonated xanthinium cations in the solid compounds, there is no evidence for protonation in DMSO-d_6 solution from the ligand ^{1}H NMR signals. Introducing a positive charge on the ring in the protonated species should induce a general downfield shift of these signals [25, 28], but they are all coincident within 0.01 ppm with those of the corresponding pure neutral ligand in the same solvent. Although protonation is not expected to produce dramatic shifts, signal coincidence indicates that the neutral species is the only form present in significant amount. Judging from the pK_a values of caffeine (0.5), theobromine (0.3) and theophylline (0.7) [28], these xanthinium ions should be very acidic, and the proton has probably been quantitatively transferred to the water present in DMSO. Consistent with this assumption is the systematic lowfield shift of the signal of residual water in the spectra of the salts. Indeed, all spectra were run under the same conditions, with the same instrument and on solutions prepared from the same batch of DMSO-d_6. For solutions of the free ligands, residual water gave a sharp signal *ca.* 3.3 ppm. With the Pd compounds, much broader signals are obtained, and they are generally displaced to the 3.6–4.1 ppm range. Dissolution of the hydrated bromopalladates

TABLE 3. Characteristic IR Bands (cm^{-1})

Compound	ν(O–H)[a]	ν(N–H)[b]	ν(C2=O)	ν(C6=O)	ν(C=C) + ν(C=N)	γ(N–H)	ν(Pd–Br)
$(TBH_2)_2PdBr_4$		2800	1687	1648	1582, 1550	851	245
$(TFH_2)_2PdBr_4$		2860	1720	1680	1575, 1555	860	251
$(CFH)PdBr_3 \cdot 7H_2O$	3405	2800	1709	1671	1574, 1551	880	247
$(TMH_2)PdBr_3 \cdot H_2O$	3461	2700	1706	1676	1605, 1572	885	253
$(ETH_2)PdBr_3 \cdot H_2O$	3470	2850	1712	1675	1650, 1570	864	249
$(PRH_2)PdBr_3 \cdot 2H_2O$	3478	2800	1708	1681	1643, 1573	883	252
$(IPH_2)PdBr_3 \cdot 2H_2O$	3494, 3400	2900	1719	1678	1569	888	256

[a]Broad absorption. [b]Broad multicomponent absorption.

TABLE 4. ^{1}H NMR Data (δ, ppm)[a]

Compound	N1–CH_3	N3–CH_3	N7–CH_3	'H_2O'	N–H	C8–R
$(TBH_2)_2PdBr_4$		3.33	3.85	5.32	11.10	7.98 (H)
$(TFH_2)_2PdBr_4$	3.24	3.44		3.70	(13.56)[b]	8.04 (H)
$(CFH)PdBr_3 \cdot 7H_2O$	3.22	3.42	3.88	3.66		8.01 (H)
$(TMH_2)PdBr_3 \cdot H_2O$	3.22	3.41		3.66	(13.17)[b]	2.37(CH_3)
$(ETH_2)PdBr_3 \cdot H_2O$	3.23	3.42		3.76	(13.16)[b]	2.71 (q, CH_2) 1.24 (t, CH_3 ^3J = 7.6[a])
$(PRH_2)PdBr_3 \cdot 2H_2O$	3.22	3.42		4.05	(13.19)[b]	2.66 (t, α-CH_2) 1.70 (m, β-CH_2, ^3J = 7.4) 0.89 (t, γ-CH_3, ^3J = 7.4)
$(IPH_2)PdBr_3 \cdot 2H_2O$	3.23	3.42		3.67	(13.11)[b]	3.04 (sp, CH) 1.27 (d, CH_3, ^3J = 7.0)

[a]In Me_2SO-d_6, 400 MHz, d = doublet, t = triplet, q = quartet, sp = septuplet, m = multiplet. [b]Resonances observed for solutions of the neutral molecules, but absent from those of the bromopalladates. [c]^3J(H–H) coupling constants in Hz.

increases the amount of water, but this cannot by itself explain the effect noted. It appears that H_3O^+ ions resulting from the dissociation of the protonated species, in fast exchange with neutral water, promote the exchange of the neutral molecule N7–H proton, whose signal was observed at 13.0–13.5 ppm for the free ligand, but is absent for the $PdBr_3$ salt. Only theobromine gives at 11.1 ppm an individual resonance for its N1–H group. It has already been noted that the N7–H groups exchange much more readily than N1–H protons in this type of molecules [29]. Therefore, our ^{1}H NMR results are consistent with complete dissociation of the xanthinium salts in solution.

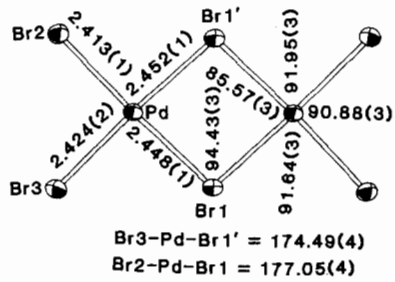

Fig. 2. ORTEP drawing of the $[Pd_2Br_6]^{2-}$ anions. Ellipsoids correspond to 50% probability. The two halves of the molecule are related by a crystallographic inversion centre in the middle of the ring.

Description of the Structure

The crystallographic work shows that the xanthine unit is not directly attached to the metal. The square planar environment of Pd is completed by formation of a dinuclear $[Pd_2Br_6]^{2-}$ unit containing two bridging Br atoms (Fig. 2). The Pd–Br bridging bonds (2.452(1) and 2.448(1) Å) are longer than those with the terminal Br ligands (2.413(1) and 2.424(2) Å). The angles around Pd are close to 90°, except for the Br1–Pd–Br1 angle in the bridging ring, which is reduced to 85.57(3)°. The environment of Pd is roughly planar, with a small, but significant, tetrahedral distortion. The atom-to-plane distances are: Pd, 0.0101(5); Br1, 0.0310(9); Br1', −0.0442(9); Br2, 0.0276(9); Br3, −0.0405(9) Å. This structure is very similar to that of the $[Pd_2Br_6]^{2-}$ ion in the tetraethylammonium salt [30].

The 1,3,8-trimethylxanthinium cation is shown in Fig. 3. In the neutral molecule, the acidic proton is probably attached to N7, as is found for theophylline [4, 31]. Therefore, the second proton in the xanthinium cation is accepted by the N9 lone pair, leading to a diprotonated five-membered ring. The geometry of the trimethylxanthinium cation

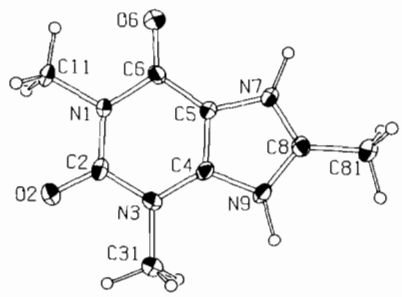

Fig. 3. ORTEP drawing of the trimethylxanthinium cation. Ellipsoids correspond to 50% probability. Hydrogens are shown as spheres of arbitrary size.

is compared with average results for related neutral molecules [8] in Table 5. Introduction of a second proton at N9 has only marginal effect on the geometry of the six-membered ring. In the N7–C8–N9 region of the neutral molecule, the N7–C8 bond is slightly longer than the C8–N9 bond. In the cation, this order is reversed (C8–N9 = 1.353(9), C8–N7 = 1.319(9) Å), indicating that the double bond is now more localized between N7 and C8. Ring angles

TABLE 5. Interatomic Distances and Bond Angles in the $(TMH_2)^+$ Cation Compared with Average Values for Similar Systems

	$(TMH_2)^+$ this work	Neutral ring[a]
Distances (Å)		
N1–C11	1.458(10)	1.479(10)
N1–C2	1.392(10)	1.398(13)
N1–C6	1.412(9)	1.398(14)
C2–N3	1.361(10)	1.371(11)
C2–O2	1.232(9)	1.214(12)
N3–C31	1.473(11)	1.470(16)
N3–C4	1.368(9)	1.378(16)
C4–C5	1.363(10)	1.362(14)
C5–C6	1.399(10)	1.415(13)
C6–O6	1.224(9)	1.229(12)
C5–N7	1.393(9)	1.385(16)
N7–C8	1.319(9)	1.346(18)
C8–N9	1.353(9)	1.337(12)
N9–C4	1.360(9)	1.352(16)
C8–C81	1.480(10)	
Angles (°)		
C11–N1–C2	117.0(6)	115.8(12)
C11–N1–C6	117.3(6)	117.6(10)
C2–N1–C6	125.5(6)	126.5(6)
N1–C2–N3	118.3(6)	116.9(12)
N1–C2–O2	119.6(7)	121.5(7)
N3–C2–O2	122.1(7)	121.6(9)
C2–N3–C31	121.6(7)	119.6(7)
C2–N3–C4	118.6(6)	119.8(9)
C4–N3–C31	119.6(6)	120.6(7)
N3–C4–C5	122.5(6)	121.5(3)
N3–C4–N9	128.3(6)	126.3(7)
C5–C4–N9	109.2(6)	112.2(7)
C4–C5–C6	122.9(7)	123.0(10)
C4–C5–N7	105.4(6)	105.4(10)
C6–C5–N7	131.6(7)	131.6(8)
C5–C6–O6	128.4(7)	127.0(7)
C5–C6–N1	112.2(6)	112.2(11)
N1–C6–O6	119.5(7)	120.9(9)
C5–N7–C8	108.8(6)	105.8(8)
N7–C8–N9	109.4(6)	113.1(8)
C8–N9–C4	107.1(6)	103.4(8)
N7–C8–C81	125.0(6)	
N9–C8–C81	125.6(6)	

[a]Average value for 14 structures of neutral xanthine derivatives containing an N7–H or N7–C bond [8].

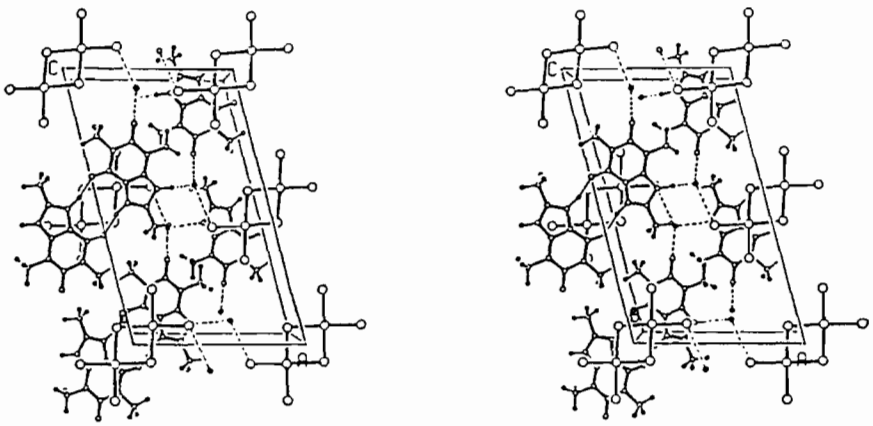

Fig. 4. View of the unit cell down the *b* axis. Atoms can be identified by reference to Figs. 2 and 3. Dotted lines correspond to hydrogen bonds. Water molecule O10 (dark spheres) can be identified between the columns of $[Pd_2Br_6]^{2-}$ and 1,3,8-trimethylxanthinium ions, by its environment of three hydrogen bonds.

usually respond to a greater extent to proton exchange. As can be seen from Table 5, introducing a proton at N9 increases the angle at N9 by 3.7°, whereas the adjacent angles at C8 and C4 are decreased by 3.7 and 3.0°, respectively. The more remote angle at N7 also undergoes a change of +3.0°. Angle variations of this magnitude, which are similar to those found upon protonation of caffeine [32], are well documented for purines [33].

A packing diagram is shown in Fig. 4. The $[Pd_2Br_6]^{2-}$ anions roughly parallel to the *ac* plane occupy crystallographic inversion centres at the cell origin and the middle of the *bc* face. Just above and below these anions are found pairs of centrosymmetrically related trimethylxanthinium cations, forming strong complementary N7–H···O6 hydrogen bonds of 2.667(8) Å. Pairs of xanthinium cations and $[Pd_2Br_6]^{2-}$ anions are stacked in alternance along the *b* direction, defining infinite columns centered on the *b* axis and the parallel direction at $z = 1/2$. Between these columns, water molecules fill channels parallel to *b* and intersecting the *ac* face at $x = 1/2$, $z = 1/2$

and $x = 1/2$, $z = 0$. Efficient use is made of the hydrogen bonding potential of water molecule O10: it acts as the acceptor for a N9–H···O10 bond of 2.714(8) Å, and as the donor toward O2 at 2.793(8) Å and Br3 at 3.311(5) Å. Br1 and Br2 are in contact with methyl hydrogens only and do not participate in significant hydrogen bonding interactions.

Supplementary Material

Tables of anisotropic temperature factors and structure factors can be obtained upon request from A.L.B.

Acknowledgements

We wish to thank the Natural Sciences and Engineering Research Council of Canada for financial support. J.M.S.P. thanks the Ministerio de Educacion y Ciencia for financial support.

References

1 D. J. Hodgson, *Prog. Inorg. Chem., 23* (1977) 211.
2 J. R. Lusty and P. F. Lee, *Inorg. Chim. Acta, 91* (1984) L47.
3 R. E. Cramer, D. M. Ho, W. V. Doorne, J. A. Ibers, T. Norton and M. Kashiwagi, *Inorg. Chim., 20* (1981) 2457.
4 D. J. Sutor, *Acta Crystallogr., 11* (1958) 83.
5 L. G. Marzilli, T. J. Kistenmacher and C. H. Chang, *J. Am. Chem. Soc., 95* (1973) 7507; L. G. Marzilli, T. J. Kistenmacher, P. E. Darcy, D. J. Szalda and M. Beer, *J. Am. Chem. Soc., 96* (1974) 4686; T. J. Kistenmacher, *Acta Crystallogr., Sect. B, 31* (1975) 85; T. J. Kistenmacher and D. J. Szalda, *Acta Crystallogr., Sect. B, 31* (1975) 90; T. J. Kistenmacher, D. J. Szalda and L. G. Marzilli, *Inorg. Chem., 14* (1975) 1686; T. Sorrell, L. G. Marzilli and T. J. Kistenmacher, *J. Am. Chem. Soc., 98* (1976) 2181; D. J. Szalda, T. J. Kistenmacher and L. G. Marzilli, *Inorg. Chem., 15* (1976) 2783; T. J. Kistenmacher and L. G. Marzilli, *Inorg. Chem., 15* (1976) 2783; T. J. Kistenmacher, D. J. Szalda, C. C. Chiang, M. Rossi and L. G. Marzilli, *Inorg. Chem., 17* (1978) 2582.
6 M. J. Gardner, F. X. Smith and E. Shefter, *J. Pharm. Sci., 72* (1983) 348.
7 A. R. Norris, S. E. Taylor, E. Buncel, F. Bélanger-Gariépy and A. L. Beauchamp, *Inorg. Chim. Acta, 92* (1984) 271; A. R. Norris, R. Kumar, E. Buncel and A. L. Beauchamp, *J. Inorg. Biochem., 21* (1984) 277; E. Buncel, R. Kumar, A. R. Norris and A. L. Beauchamp, *Can. J. Chem., 63* (1985) 2575.
8 D. Cozak, A. Mardhy, M. J. Olivier and A. L. Beauchamp, *Inorg. Chem., 25* (1986) 2600.
9 D. J. Sutor, *Acta Crystallogr., 11* (1958) 453.
10 M. B. Cingi, A. M. M. Lanfredi, A. Tiripicchio, G. Bandoli and D. A. Clemente, *Inorg. Chim. Acta, 52* (1981) 237.
11 F. Allaire and A. L. Beauchamp, *Can. J. Chem., 62* (1984) 2249.
12 M. A. Romero-Molina, E. Colacio-Rodriguez, J. Ruiz-Sanchez, J. M. Salas-Peregrin and F. Nieto, *Inorg. Chim. Acta, 123* (1986) 133.
13 C. M. Mikulski, T. B. Tran, L. Mattucci and N. M. Karayannis, *Inorg. Chim. Acta, 78* (1983) 211.
14 E. Colacio-Rodriguez, J. D. Lopez-Gonzalez and J. M. Salas-Peregrin, *Can. J. Chem., 61* (1983) 2506.
15 J. R. Lusty, H. S. O. Chan, E. Khor and J. Peeling, *Inorg. Chim. Acta, 106* (1985) 209.
16 C. M. Mikulski, M. K. Kurlan and N. M. Karayannis, *Inorg. Chim. Acta, 106* (1985) L25.
17 C. M. Mikulski, M. K. Kurlan, M. Bayne, M. Gaul and N. M. Karayannis, *Inorg. Chim. Acta, 123* (1986) 27, and refs. therein.
18 J. M. Salas-Peregrin, E. Colacio-Rodriguez, M. A. Romero-Molina and M. P. Sanchez-Sanchez, *Thermochim. Acta, 69* (1983) 313.
19 J. M. Salas-Peregrin, E. Colacio-Rodriguez, M. Moreno-Carretero and J. D. Lopez-Gonzalez, *An. Quim., 80B* (1984) 167; J. M. Salas-Peregrin, E. Sanchez-Martinez and E. Colacio-Rodriguez, *Inorg. Chim. Acta, 107* (1985) 23; E. Colacio-Rodriguez, J. M. Salas-Peregrin, J. Ruiz-Sanchez and E. Garcia-Megias, *Thermochim. Acta, 89* (1985) 159; E. Colacio-Rodriguez, J. M. Salas-Peregrin, R.. Lopez-Garzon and J. D. Lopez-Gonzalez, *Thermochim. Acta, 71* (1983) 139; E. Colacio-Rodriguez, J. D. Lopez-Gonzalez and J. M. Salas-Peregrin, *J. Thermal. Anal., 28* (1983) 3.
20 F. Colacio-Rodriguez, J. M. Salas-Peregrin and J. D. Lopez-Gonzalez, *An. Quim., 80B* (1984) 223; E. Colacio-Rodriguez and J. M. Salas-Peregrin, *Thermochim. Acta, 74* (1984) 45; E. Colacio-Rodriguez, M. N. Moreno-Carretero and J. M. Salas-Peregrin, *J. Thermal. Anal., 30* (1985) 771; M. N. Moreno-Carretero, E. Colacio-Rodriguez, J. M. Salas-Peregrin and M. P. Sanchez-Sanchez, *An. Quim., 81B* (1985) 313; M. N. Moreno-Carretero, E. Colacio-Rodriguez and J. M. Salas-Peregrin, *Thermochim. Acta, 97* (1986) 67.
21 J. H. Speer and A. L. Raymond, *J. Am. Chem. Soc., 75* (1953) 114.
22 F. Bélanger-Gariépy and A. L. Beauchamp, *J. Am. Chem. Soc., 102* (1980) 3461.
23 G. M. Sheldrick, *SHELX-76*, system of computer programs, University of Cambridge, U.K.
24 D. T. Cromer and J. T. Waber, *Acta Crystallogr., 18* (1965) 104; R. F. Stewart, E. R. Davidson and W. T. Simpson, *J. Chem. Phys., 42* (1965) 3175; D. T. Cromer, *Acta Crystallogr., 18* (1965) 17.
25 D. Cook and Z. R. Regnier, *Can. J. Chem., 45* (1967) 2895.
26 D. Cook and Z. R. Regnier, *Can. J. Chem., 45* (1967) 2900.
27 J. R. Ferraro, *Low-frequency Vibration of Inorganic and Coordination Compounds*, Plenum, New York, 1971; P. L. Goggin and J. Mink, *Inorg. Chim. Acta, 26* (1978) 119; *J. Chem. Soc., Dalton Trans.*, (1974) 1479.
28 D. Lichtenberg, F. Bergmann and Z. Neiman, *J. Chem. Soc. C*, (1971) 1676; (1971) 1939.
29 L. M. Twanmoh, H. B. Wood, Jr. and J. S. Driscoll, *J. Heterocycl. Chem., 10* (1973) 187.
30 D. R. Russell, P. A. Tucker and C. Whittaker, *Acta Crystallogr., Sect. B, 31* (1975) 2530.
31 K. Aoki, T. Ichikawa, Y. Koinuma and Y. Iitaka, *Acta Crystallogr., Sect. B, 34* (1978) 2333; S. Nakao, S. Fujii, T. Sakaki and K. I. Tomita, *Acta Crystallogr., Sect. B, 33* (1977) 1373; E. Shefter, *J. Pharm. Sic., 58* (1969) 710.
32 A. Mercer and J. Trotter, *Acta Crystallogr., Sect. B, 34* (1978) 450.
33 R. Taylor and O. Kennard, *J. Mol. Struct., 78* (1982) 1.